

GOSPA and T-GOSPA quasi-metrics for evaluation of multi-object tracking algorithms

Ángel F. García-Fernández, Jinhao Gu, Lennart Svensson, Yuxuan Xia, Jan Krejčí, Oliver Kost, Ondřej Straka

Abstract—This paper introduces two quasi-metrics for performance assessment of multi-object tracking (MOT) algorithms. In particular, one quasi-metric is an extension of the generalised optimal subpattern assignment (GOSPA) metric and measures the discrepancy between sets of objects. The other quasi-metric is an extension of the trajectory GOSPA (T-GOSPA) metric and measures the discrepancy between sets of trajectories. Similar to the GOSPA-based metrics, these quasi-metrics include costs for localisation error for properly detected objects, the number of false objects and the number of missed objects. The T-GOSPA quasi-metric also includes a track switching cost. Differently from the GOSPA and T-GOSPA metrics, the proposed quasi-metrics have the flexibility of penalising missed and false objects with different costs, and the localisation costs are not required to be symmetric. These properties can be useful in MOT evaluation in certain applications. The performance of several Bayesian MOT algorithms is assessed with the T-GOSPA quasi-metric via simulations.

Index Terms—Metrics, GOSPA quasi-metric, multi-object tracking, performance evaluation.

I. INTRODUCTION

Multi-object tracking (MOT) consists of estimating the trajectories of a variable and an unknown number of objects using sensor measurements. MOT has a wide variety of applications such as traffic monitoring [1], underwater surveillance [2], and space object cataloging [3]. This paper considers an important topic of MOT, which is how to evaluate the performance of MOT algorithms [4], [5]. That is, given a ground truth set of trajectories, and the estimated sets of trajectories provided by several algorithms, the best performing algorithm is the one whose estimate is the most similar to the ground truth. Therefore, to assess MOT algorithm performance, it is necessary to establish a definition of error or distance between two sets of trajectories.

In mathematics, the notion of error or distance can be defined via metrics¹. Metrics are non-negative functions that

meet three properties: identity, symmetry, and triangle inequality [6]. These properties ensure that the notion of distance is intuitive and they are the foundation of important properties for mathematical analysis, such as the concept of metric spaces. The triangle inequality guarantees that distances between points follow a consistent and logical pattern. That is, it prevents cases where the direct distance between two endpoints is greater than the sum of the distances between any intermediate points. We proceed to review the literature on performance evaluation for MOT.

Multi-object filtering is a sub-problem of MOT in which the goal is to estimate the current set of objects, rather than the set of trajectories. A widely-used metric for sets of objects is the optimal sub-pattern assignment (OSPA) metric [7], [8]. Other metrics for sets of objects are the cardinalised optimal linear assignment metric [9], [10], which is proportional to the unnormalised OSPA metric, the Hausdorff and Wasserstein metrics [11], and the complete OSPA metric [12]. However, none of the above mentioned metrics penalise all the factors that are considered of interest in MOT: localisation errors for detected objects, the number of missed objects and the number of false objects. These can be penalised with the generalised optimal sub-pattern assignment (GOSPA) metric [13].

In MOT, apart from penalising the above factors, it is relevant to penalise track switches, in which the estimated trajectories of different objects are swapped at some point in time. In computer vision, there are several ways to penalise track switches. One example is the multiple object tracking accuracy (MOTA) score [14], and its variations [15]. MOTA is based on obtaining a heuristic matching between the ground truth states and the estimated object states at each time step. With this matching, the MOTA score is defined based on the number of track switches, missed and false objects, but not on the localisation errors for matched objects [14]. The MOTA score indicates similarity, takes values in the interval $(-\infty, 1]$, and is non-symmetric. As MOTA does not consider localisation errors, these are usually measured in this setting by calculating a companion index, the multiple object tracking precision (MOTP). The MOTP was originally defined as an error [14], but it can also be defined as a similarity with a minor modification [16].

Another similarity score for MOT used in computer vision, taking values in $[0, 1]$, is the higher order tracking accuracy (HOTA) score [16]. The HOTA score for a given similarity threshold α (HOTA_α) is based on solving an external assignment problem (e.g., an assignment problem with another cost function) at each time step. The solutions of the external assignment problems are then used to calculate

A. F. García-Fernández is with the IPTC, ETSI de Telecomunicación, Universidad Politécnica de Madrid, 28040 Madrid, Spain (email: angel.garcia.fernandez@upm.es).

J. Gu is with Department of Electrical Engineering and Electronics, University of Liverpool, Liverpool L69 3GJ (email: jinhgu@liverpool.ac.uk).

L. Svensson is with the Department of Electrical Engineering, Chalmers University of Technology, SE-412 96 Gothenburg, Sweden (email: lennart.svensson@chalmers.se).

Y. Xia is with the Department of Automation and Intelligent Sensing, Shanghai Jiao Tong University, Shanghai, China (e-mail: yuxuan.xia@sjtu.edu.cn).

J. Krejčí, O. Kost, O. Straka are with the Department of Cybernetics, University of West Bohemia, Pilsen, Czech Republic (e-mails: {jkrejci, kost, straka30}@kky.zcu.cz).

¹The terms distance and metric are sometimes used interchangeably. In this paper, a distance refers to a function that may not fulfill all the mathematical properties required of a metric.

the HOTA_α score, which depends on the number of missed objects, false objects and track switches, but it does not depend on localisation errors for properly detected objects. The overall HOTA is then obtained by summing HOTA_α over multiple similarity thresholds, to indirectly account for localisation errors. However, none of MOTA, MOTP or HOTA are mathematical metrics, as they do not meet the identity and triangle inequality properties. Moreover, MOTA is not symmetric and does not have the required range.

To define a metric for sets of trajectories, one solution is to first determine a base distance for trajectories and then apply the OSPA metric. This procedure results in the $\text{OSPA}^{(2)}$ metric [17]. This metric associates estimated trajectories to ground truth trajectories, but the association remains fixed across time. Therefore, the $\text{OSPA}^{(2)}$ metric does not include penalties for track switches, and it does not penalise the number of missed and false objects, either [18]. Bento's metrics are mathematically consistent metrics for sets of trajectories and penalise track switches, though they require the introduction of \ast -trajectories to ensure the two sets have the same number of elements [19]. The extension of the GOSPA metric for sets of trajectories, termed trajectory GOSPA (T-GOSPA) metric, was presented in [20] to penalise localisation errors, the number of missed and false objects, and the number of track switches. T-GOSPA works by assigning at each time step trajectories in both sets, while allowing for the possibility of leaving trajectories unassigned. T-GOSPA was extended to have time-weighted costs in [18]. Both T-GOSPA and Bento's metrics have linear programming (LP) relaxation variants, which are also metrics and are faster to compute. An approximate, fast implementation of the T-GOSPA metric for large tracking scenarios based on unbalanced multimarginal optimal transport problem has been recently proposed in [21].

A property of the GOSPA and T-GOSPA metrics is that missed and false objects are penalised with the same cost, to ensure the symmetry property. The previous distances and similarity scores also share this property. However, there are some applications in which it is more suitable to have different costs for missed and false objects. For instance, in classic radar detector design, one typically sets a very low probability of false alarm and then maximises the probability of detection using a Neyman-Pearson test [22, Chap. 10]. With this design, the cost of a false object is higher than the cost of a missed object. In other applications, such as self-driving vehicles, it is crucial not to miss any objects. Hence, it is desirable to assess algorithms with a higher penalty for missed objects than for false objects.

To achieve this flexibility in the costs for missed and false objects, it is necessary to develop distance functions that are non-symmetric. Distances that meet the metric properties except the symmetry property are called quasi-metrics (q-metrics) [23]–[25]. Q-metrics have been used in several applications: similarity search in protein datasets [26], reinforcement learning [27], and q-metric learning [28]. Suitable q-metrics for MOT should also penalise the aspects of interest in MOT: localisation errors, number of false objects, number of missed objects, and track switches. This paper fills in this gap in the literature by proposing the GOSPA and T-GOSPA

q-metrics. These q-metrics are designed based on the GOSPA and T-GOSPA metrics by using a base distance that is a q-metric and incorporating an additional parameter $\rho \in (0, 1)$ that controls the penalties for false and missed objects.

The contributions of this paper are:

- Development of the GOSPA q-metric² for sets of objects for performance evaluation of multi-object filters with different costs for missed and false objects, including the proofs of the q-metric properties.
- Development of the T-GOSPA q-metric for sets of trajectories for performance evaluation of MOT algorithms with different costs for missed and false objects, including the proofs of the q-metric properties.
- Derivation of three properties of the GOSPA and T-GOSPA q-metrics related to the q-metric parameter ρ .
- Extensions of the GOSPA and T-GOSPA q-metrics to random finite sets (RFSs) [29].

The paper also provides simulation results evaluating state-of-the-art Bayesian MOT algorithms via the T-GOSPA q-metric.

The organisation of the remainder of the paper is as follows. Section II presents the required background. Sections III and IV introduce the GOSPA and T-GOSPA q-metrics, respectively. The extensions of the q-metrics to RFSs are provided in Section V. Simulation results are analysed via the T-GOSPA q-metric in Section VI. Section VII gives the conclusions.

II. BACKGROUND

This section introduces the variables we consider (Section II-A), the definitions of metrics and q-metrics (Section II-B), and the GOSPA metric (Section II-C).

A. Variables

We denote a single object state as $x \in \mathbb{X}$, with \mathbb{X} being the single-object space. The single-object space is typically $\mathbb{X} = \mathbb{R}^{n_x}$, and contains information on the object dynamics such as position and velocity, and it can also include discrete variables such as object type. A set of objects is then represented as $\mathbf{x} = \{x_1, \dots, x_{n_x}\}$, and its cardinality is $|\mathbf{x}| = n_x$ [29].

The trajectory of an object is denoted by $X = (\omega, x^{1:\nu})$. Here, ω is the trajectory start time step, ν is the trajectory duration and $x^{1:\nu} = (x^1, \dots, x^\nu)$ is the sequence of object states of this trajectory [30]. We focus on trajectories contained in a time window from time step 1 to time step T , such that $1 \leq \omega \leq T$ and $1 \leq \nu \leq T - \omega + 1$. A set of object trajectories is denoted by $\mathbf{X} = \{X_1, \dots, X_{n_x}\}$, with its cardinality being $|\mathbf{X}| = n_x$.

B. Metric and q-metrics

A metric on a given space Υ is a non-negative function $d(\cdot, \cdot) : \Upsilon \times \Upsilon \rightarrow [0, \infty)$ that meets the following three properties for any $\mathbf{X}, \mathbf{Y}, \mathbf{Z} \in \Upsilon$ [6]

- $d(\mathbf{X}, \mathbf{Y}) = 0$ if and only if $\mathbf{X} = \mathbf{Y}$ (identity),
- $d(\mathbf{X}, \mathbf{Y}) = d(\mathbf{Y}, \mathbf{X})$ (symmetry),

²Matlab and Python implementations of the GOSPA and T-GOSPA q-metrics will be publicly shared after publication.

- $d(\mathbf{X}, \mathbf{Y}) \leq d(\mathbf{X}, \mathbf{Z}) + d(\mathbf{Z}, \mathbf{Y})$ (triangle inequality).

A q-metric is a non-negative function $d(\cdot, \cdot) : \Upsilon \times \Upsilon \rightarrow [0, \infty)$ that meets the identity and triangle inequality properties, but it does not need to meet the symmetry property [23]–[25].

The triangle inequality is a key property to define distances between points in a space, and also to measure the error of estimators. For example, let us illustrate this with the following example, adapted from [29, Sec. 6.2.1]. Let \mathbf{X} be the ground truth and let \mathbf{Y}_1 and \mathbf{Y}_2 be two estimates. If estimate \mathbf{Y}_1 is close to \mathbf{X} and estimate \mathbf{Y}_2 is close to \mathbf{Y}_1 , that is, both $d(\mathbf{X}, \mathbf{Y}_1)$ and $d(\mathbf{Y}_1, \mathbf{Y}_2)$ are small, then \mathbf{Y}_2 should be close to \mathbf{X} implying that $d(\mathbf{X}, \mathbf{Y}_2)$ is small as well. This property is ensured for metrics and q-metrics by the triangle inequality.

In this rest of this paper, the ground truth set of objects and the ground truth set of trajectories are denoted by \mathbf{x} and \mathbf{X} . The corresponding estimates provided by a certain algorithm are denoted by \mathbf{y} and \mathbf{Y} .

C. GOSPA metric

This subsection reviews the GOSPA metric (for parameter $\alpha = 2$, as defined in [13]), as it is the point of reference for the q-metrics. The ground truth sets of objects and its estimate are written as $\mathbf{x} = \{x_1, \dots, x_{n_x}\}$ and $\mathbf{y} = \{y_1, \dots, y_{n_y}\}$. The GOSPA metric looks for an optimal assignment set between the objects in \mathbf{x} and the elements in \mathbf{y} , with the assignment set indicating what objects are matched, and which ones are left without assignment. An assignment set θ meets $\theta \subseteq \{1, \dots, n_x\} \times \{1, \dots, n_y\}$ and, $(i, j), (i, j') \in \theta$ implies $j = j'$ and, $(i, j), (i', j) \in \theta$ implies $i = i'$. The set of all possible assignment sets is denoted by $\Gamma_{\mathbf{x}, \mathbf{y}}$, such that $\theta \in \Gamma_{\mathbf{x}, \mathbf{y}}$.

Definition 1. For a base metric $d_b(\cdot, \cdot)$ on the single-object space \mathbb{X} , a maximum localisation cost parameter $c > 0$, and a real parameter p with $1 \leq p < \infty$, the GOSPA metric between sets \mathbf{x} and \mathbf{y} of objects is [13, Prop. 1]

$$d_p^{(c)}(\mathbf{x}, \mathbf{y}) = \min_{\theta \in \Gamma_{\mathbf{x}, \mathbf{y}}} \left(\sum_{(i, j) \in \theta} d_b(x_i, y_j)^p + \frac{c^p}{2} (|\mathbf{x}| + |\mathbf{y}| - 2|\theta|) \right)^{1/p}. \quad (1)$$

The first term in (1) is the sum of the localisation costs (to the p -th power) for pairs of assigned objects, whose indices $(i, j) \in \theta$. These are the objects in \mathbf{x} that have been properly detected and, therefore, have an associated object in the estimated set \mathbf{y} . The terms $\frac{c^p}{2} (|\mathbf{x}| - |\theta|)$ and $\frac{c^p}{2} (|\mathbf{y}| - |\theta|)$ are the penalties (to the p -th power) for the number of missed and false objects. Each missed and each false object contributes with an cost $\frac{c^p}{2}$ to the overall cost (before we take the p -th root).

III. GOSPA Q-METRIC

This section introduces the GOSPA q-metric in Section III-A. Then, we present representative examples to illustrate how the q-metric works in Section III-B. The choice of parameters is explained in Section III-C. Three properties of the GOSPA q-metric are provided in Section III-D.

A. Definition

The definition of the GOSPA q-metric is the following.

Definition 2. For a base q-metric $d_b(\cdot, \cdot)$ in the single-object space \mathbb{X} , a maximum localisation cost parameter $c > 0$, real parameter p with $1 \leq p < \infty$, and q-metric parameter $\rho \in (0, 1)$, the GOSPA q-metric $d_p^{(c, \rho)}(\cdot, \cdot)$ between two sets \mathbf{x} and \mathbf{y} of objects is

$$d_p^{(c, \rho)}(\mathbf{x}, \mathbf{y}) = \min_{\theta \in \Gamma_{\mathbf{x}, \mathbf{y}}} \left(\sum_{(i, j) \in \theta} d_b^p(x_i, y_j) + \rho c^p (|\mathbf{y}| - |\theta|) + (1 - \rho) c^p (|\mathbf{x}| - |\theta|) \right)^{1/p}. \quad (2)$$

The differences between the GOSPA q-metric (2) and the GOSPA metric in (1) are that $d_b(\cdot, \cdot)$ is allowed to be a q-metric, the penalty (to the p -th power) for a false object is $c_f^p = \rho c^p$ and the penalty (to the p -th power) for a missed object is $c_m^p = (1 - \rho) c^p$, where $\rho \in (0, 1)$ is the fraction of the maximum localisation error c^p that represents a false object cost (to the p -th power). Note that for $\rho = 1/2$ and $d_b(\cdot, \cdot)$ being a metric, the GOSPA q-metric becomes the GOSPA metric.

An alternative parameterisation of the GOSPA q-metric is to define it in terms of c_f and c_m , instead of c and ρ . The conversion between both parameterisations is straightforward. We use the parameterisation in terms of c and ρ as parameter c is the maximum localisation cost that enables a pair of objects can be assigned to each other, which is an intuitive concept. Parameter c is also used in the GOSPA metric and is used in the triangle inequality proof.

It is direct to check the non-negativity and identity properties of the GOSPA q-metric. The triangle inequality is proved in Appendix A. In the proof of the triangle inequality, we use the definition of the GOSPA q-metric in terms of permutations instead of assignment sets. To use this alternative expression, we introduce the cut-off base q-metric $d^{(c)}(x, y) = \min(d_b(x, y), c)$. The set of all permutations on $\mathbb{N}_n = \{1, \dots, n\}$ is denoted by Π_n such that a permutation is written as $\pi = (\pi(1), \dots, \pi(n)) \in \Pi_n$, with $\pi(i) \in \mathbb{N}_n$, $i \in \mathbb{N}_n$.

Lemma 3. For $|\mathbf{y}| \geq |\mathbf{x}|$, the GOSPA q-metric in (2) in permutation form is

$$d_p^{(c, \rho)}(\mathbf{x}, \mathbf{y}) = \min_{\pi \in \Pi_{|\mathbf{y}|}} \left(\sum_{i=1}^{|\mathbf{x}|} d^{(c)}(x_i, y_{\pi(i)})^p + \rho c^p (|\mathbf{y}| - |\mathbf{x}|) \right)^{1/p} \quad (3)$$

and, for $|\mathbf{y}| \leq |\mathbf{x}|$, the GOSPA q-metric is

$$d_p^{(c, \rho)}(\mathbf{x}, \mathbf{y}) = \min_{\pi \in \Pi_{|\mathbf{x}|}} \left(\sum_{i=1}^{|\mathbf{y}|} d^{(c)}(y_i, x_{\pi(i)})^p + (1 - \rho) c^p (|\mathbf{x}| - |\mathbf{y}|) \right)^{1/p}. \quad (4)$$

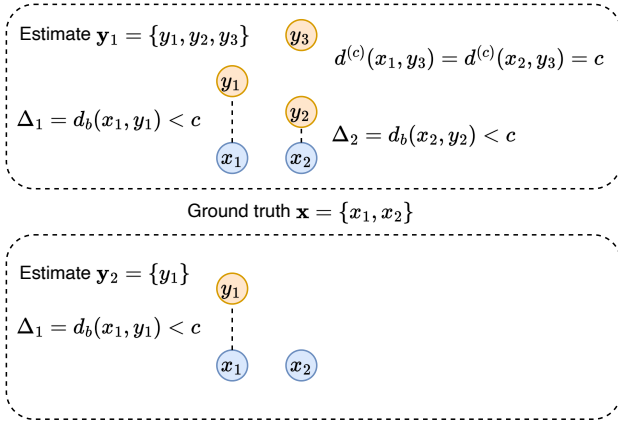


Figure 1: Two estimated sets of objects \mathbf{y}_1 and \mathbf{y}_2 of the ground truth \mathbf{x} . The dashed lines represent assignments between the elements of the ground truth and the estimate. Estimate \mathbf{y}_1 has two properly detected objects with localisation errors Δ_1 and Δ_2 and a false object. Estimate \mathbf{y}_2 has one properly detected object with localisation error Δ_1 plus a missed object.

The proof of this lemma follows the proof of how to write the GOSPA metric as an optimisation over assignment sets instead of permutations [13, App. B].

B. Examples

We demonstrate the operation of the GOSPA q-metric using the examples presented in Figure 1. For clarity, we focus on the case where $p = 1$. This results in the following q-metric values

$$d_1^{(c,\rho)}(\mathbf{x}, \mathbf{y}_1) = \Delta_1 + \Delta_2 + \rho c \quad (5)$$

$$d_1^{(c,\rho)}(\mathbf{x}, \mathbf{y}_2) = \Delta_1 + (1 - \rho) c. \quad (6)$$

For the GOSPA metric ($\rho = 1/2$), \mathbf{y}_2 is more accurate than \mathbf{y}_1 . For the GOSPA q-metric, the estimate \mathbf{y}_2 is more accurate than \mathbf{y}_1 if

$$\rho > \frac{1}{2} - \frac{\Delta_2}{2c}. \quad (7)$$

That is, the parameter ρ , which is proportional to the false object cost, must be sufficiently high such that \mathbf{y}_2 is considered better than \mathbf{y}_1 . This is intuitive as \mathbf{y}_2 misses an object while \mathbf{y}_1 has a false object and one more estimate associated to a true object, so high enough false object penalties makes \mathbf{y}_2 a better estimate. On the contrary, for sufficiently small ρ , the GOSPA q-metric indicates that \mathbf{y}_1 is more accurate than \mathbf{y}_2 , since the false object is penalised less.

Let us now consider the case where $\Delta_1 > c$ and $\Delta_2 > c$. In this case, the optimal assignments are not the ones shown in Figure 1 as it is best to leave all objects unassigned. This implies that \mathbf{y}_1 misses two objects and declares three false objects. On the other hand, \mathbf{y}_2 misses two objects and contains one false object. This results in the GOSPA q-metric values $d_1^{(c,\rho)}(\mathbf{x}, \mathbf{y}_1) = 2c + \rho c$ and $d_1^{(c,\rho)}(\mathbf{x}, \mathbf{y}_2) = c + (1 - \rho) c$. In this case, \mathbf{y}_2 is more accurate than \mathbf{y}_1 for all values of $\rho \in (0, 1)$. This is intuitive as now \mathbf{y}_1 and \mathbf{y}_2 miss the same number of objects, but \mathbf{y}_1 has three false objects and \mathbf{y}_2 only one false object.

C. Choice of parameters

The parameters c and p are chosen as in the GOSPA metric. That is, parameter c is the maximum localisation error and is chosen depending on the application. One true object state x and an estimate y can only be assigned to each other if their distance according to the base q-metric is lower than c . Parameter p can be chosen to adapt how outliers are penalised, with a higher value of p penalising outliers more [8], [13].

In most applications, the base q-metric $d_b(\cdot, \cdot)$ will typically be chosen to be a metric. For example, for point objects (which do not have an extent), one can use the Euclidean distance. For extended objects modelled by ellipses, one can use the Gaussian Wasserstein distance [31]. Parameter ρ can be chosen taking into account how much a false object should be penalised compared to a missed object in a given application. This leads to the following lemma.

Lemma 4. *If the cost of a false object (to the p -th power), is $\nu \in (0, \infty)$ times the cost (to the p -th power) of a missed object ($c_f^p = \nu c_m^p$), the GOSPA q-metric parameter ρ is*

$$\rho = \frac{\nu}{\nu + 1}. \quad (8)$$

The proof this lemma follows from the definitions of c_f^p and c_m^p in the paragraph after (2).

D. Properties

This section provides several properties of the GOSPA q-metric. Straight from the definition, it is direct to prove the following lemma.

Lemma 5. *If $d_b(\cdot, \cdot)$ is a metric, the GOSPA q-metric meets*

$$d_p^{(c,\rho)}(\mathbf{x}, \mathbf{y}) = d_p^{(c,1-\rho)}(\mathbf{y}, \mathbf{x}). \quad (9)$$

In addition, we prove in Appendix B-A the following result.

Lemma 6. *The optimal assignment set (or the optimal permutation) of the GOSPA q-metric does not depend on ρ .*

This result implies that for different values of ρ , the localisation costs remain unchanged, but we have different missed and false object costs, and a different overall metric value. In addition, Lemma 6 implies that, if $d_b(\cdot, \cdot)$ is a metric, the optimal assignment set is the same as in the GOSPA metric.

The symmetrisation property of the GOSPA q-metric is stated in the following lemma (proved in Appendix B-B).

Lemma 7. *If $d_b(\cdot, \cdot)$ is a metric, the GOSPA metric $d_p^{(c,1/2)}(\mathbf{x}, \mathbf{y})$ is recovered with the following symmetrisation of the GOSPA q-metric*

$$d_p^{(c,1/2)}(\mathbf{x}, \mathbf{y}) = \left[\frac{1}{2} \left(d_p^{(c,\rho)}(\mathbf{x}, \mathbf{y})^p + d_p^{(c,\rho)}(\mathbf{y}, \mathbf{x})^p \right) \right]^{1/p}. \quad (10)$$

IV. T-GOSPA Q-METRICS

This section presents the T-GOSPA q-metrics for sets of trajectories. We first cover the GOSPA q-metric for sets of objects with at most one element (Section IV-A). We then present the T-GOSPA q-metric for sets of trajectories in terms

of multi-dimensional assignments across time (Section IV-B). Then, we introduce the relaxation of the multi-dimensional assignment T-GOSPA q-metric via linear programming (Section IV-C). Examples illustrating the T-GOSPA q-metric results are presented in Section IV-D. Finally, three properties of the T-GOSPA q-metrics are presented (Section IV-E).

A. Preliminaries

A building block of the T-GOSPA q-metric is the GOSPA q-metric for sets of objects with at most one element. Given two sets of objects \mathbf{x} and \mathbf{y} such that $|\mathbf{x}| \leq 1$ and $|\mathbf{y}| \leq 1$, the GOSPA q-metric (2) becomes

$$d_p^{(c,\rho)}(\mathbf{x}, \mathbf{y}) \triangleq \begin{cases} \min(c, d_b(x, y)) & \mathbf{x} = \{x\}, \mathbf{y} = \{y\} \\ \rho^{1/p} c & \mathbf{x} = \emptyset, \mathbf{y} = \{y\} \\ (1 - \rho)^{1/p} c & \mathbf{x} = \{x\}, \mathbf{y} = \emptyset \\ 0 & \mathbf{x} = \mathbf{y} = \emptyset. \end{cases} \quad (11)$$

B. Multi-dimensional assignment T-GOSPA q-metric

This section presents the T-GOSPA q-metric as the solution to a multi-dimensional assignment problem. The ground truth sets of trajectories and its estimate are written as $\mathbf{X} = \{X_1, \dots, X_{n_{\mathbf{X}}}\}$ and $\mathbf{Y} = \{Y_1, \dots, Y_{n_{\mathbf{Y}}}\}$. For the trajectories X_i and Y_j , the corresponding set of objects at time step k are represented by \mathbf{x}_i^k and \mathbf{y}_j^k . It is met that $|\mathbf{x}_i^k| \leq 1$ and $|\mathbf{y}_j^k| \leq 1$ as these sets are either empty, if the corresponding trajectory does not have an object state at time step k , or have a single element. The number of objects in \mathbf{X} that are present at time step k is denoted $n_{\mathbf{X}}^k = \sum_{i=1}^{n_{\mathbf{X}}} |\mathbf{x}_i^k|$. A similar notation, $n_{\mathbf{Y}}^k$, is used for \mathbf{Y} .

In the trajectory q-metrics, we make assignments at each time step between the trajectories in \mathbf{X} and those in \mathbf{Y} . That is, at each time step, each set \mathbf{x}_i^k is associated to a set \mathbf{y}_j^k or is left without an assignment.

To represent these assignments, we can use assignment vectors as follows. An assignment vector at time step k is written as $[\pi_1^k, \dots, \pi_{n_{\mathbf{X}}}^k]$, with $n_{\mathbf{X}}$ being its length. If its i -th entry $\pi_i^k = j$, with $j \in \{1, \dots, n_{\mathbf{Y}}\}$, it means that \mathbf{x}_i^k is assigned to \mathbf{y}_j^k . As there can be at maximum one \mathbf{x}_i^k assigned to \mathbf{y}_j^k , and the other way round, the assignment vector has the constraint that $\pi_i^k = \pi_{i'}^k = j > 0$ implies $i = i'$. A value $\pi_i^k = 0$ implies that \mathbf{x}_i^k is unassigned. The set of all these possible assignment vectors is then written as $\Pi_{\mathbf{X}, \mathbf{Y}}$.

Definition 8. Given a base q-metric $d_b(\cdot, \cdot)$ in the single-object space \mathbb{X} , a maximum localisation cost $c > 0$, a real parameter p with $1 \leq p < \infty$, a track switching penalty $\gamma > 0$, and q-metric parameter $\rho \in (0, 1)$, the T-GOSPA q-metric $d_p^{(c,\rho,\gamma)}(\mathbf{X}, \mathbf{Y})$ between two sets \mathbf{X} and \mathbf{Y} of trajectories is

$$d_p^{(c,\rho,\gamma)}(\mathbf{X}, \mathbf{Y}) = \min_{\pi^k \in \Pi_{\mathbf{X}, \mathbf{Y}}} \left(\sum_{k=1, \dots, T} d_{\mathbf{X}, \mathbf{Y}}^k(\mathbf{X}, \mathbf{Y}, \pi^k)^p + \sum_{k=1}^{T-1} s_{\mathbf{X}, \mathbf{Y}}(\pi^k, \pi^{k+1})^p \right)^{1/p} \quad (12)$$

where

$$d_{\mathbf{X}, \mathbf{Y}}^k(\mathbf{X}, \mathbf{Y}, \pi^k)^p = \sum_{(i,j) \in \theta^k(\pi^k)} d_p^{(c,\rho)}(\mathbf{x}_i^k, \mathbf{y}_j^k)^p + \rho c^p (n_{\mathbf{X}}^k - |\theta^k(\pi^k)|) + (1 - \rho) c^p (n_{\mathbf{Y}}^k - |\theta^k(\pi^k)|) \quad (13)$$

includes the costs (to the p -th power) for properly detected objects (first line), false objects (second line) and missed objects (third line) at time step k , $d_p^{(c,\rho)}(\cdot, \cdot)$ is the GOSPA q-metric in (11),

$$\theta^k(\pi^k) = \left\{ (i, \pi_i^k) : i \in \{1, \dots, n_{\mathbf{X}}\}, |\mathbf{x}_i^k| = |\mathbf{y}_{\pi_i^k}^k| = 1, d_p^{(c,\rho)}(\mathbf{x}_i^k, \mathbf{y}_{\pi_i^k}^k) < c \right\} \quad (14)$$

and the track switch penalty (to the p -th power) between time step k and $k + 1$ is

$$s_{\mathbf{X}, \mathbf{Y}}(\pi^k, \pi^{k+1})^p = \gamma^p \sum_{i=1}^{n_{\mathbf{X}}} s(\pi_i^k, \pi_i^{k+1}) \quad (15)$$

$$s(\pi_i^k, \pi_i^{k+1}) = \begin{cases} 0 & \pi_i^k = \pi_i^{k+1} \\ 1 & \pi_i^k \neq \pi_i^{k+1}, \pi_i^k \neq 0, \pi_i^{k+1} \neq 0 \\ \frac{1}{2} & \text{otherwise.} \end{cases}$$

The proof that Definition 8 is a q-metric, meeting the properties indicated in Section II-B, will be included as part of the proof for its linear programming version in the next subsection. The T-GOSPA q-metric above (and also the linear programming relaxation version in the next subsection) are simply using the GOSPA q-metric (11) inside the original T-GOSPA metric in [20]. The T-GOSPA metric is obtained by setting $\rho = 1/2$ provided that $d_b(\cdot, \cdot)$ is a metric. Apart from the costs for false, missed and localization errors (already present in the GOSPA q-metric), the T-GOSPA q-metric also introduces a cost for track switches that remains symmetric in the q-metric, to enable the linear programming relaxation. Equation (13) corresponds to the GOSPA q-metric, but with the object-level assignment set $\theta^k(\pi^k)$ being determined by the trajectory-level association π^k . For two objects to be assigned in $\theta^k(\pi^k)$, their base q-metric must be smaller than c , as indicated by (14). For one time step $T = 1$, the T-GOSPA q-metric becomes the GOSPA q-metric. Parameter ρ is the T-GOSPA q-metric can be chosen as in the GOSPA q-metric, see Section III-C. The rest of the parameters can be chosen as in the T-GOSPA metric [20].

C. Linear programming T-GOSPA q-metric

To define the linear programming T-GOSPA q-metric, we first need to provide some additional notation. The transpose of a matrix A is written as A^\top . The assignments of the T-GOSPA q-metric can be written using binary matrices [20]. A matrix W^k of size $(n_{\mathbf{X}} + 1) \times (n_{\mathbf{Y}} + 1)$ that represents assignments between \mathbf{X} and \mathbf{Y} meets the properties:

$$W^k(i, j) \in \{0, 1\}, \forall i, j \quad (16)$$

$$\sum_{i=1}^{n_{\mathbf{X}}+1} W^k(i, j) = 1, \quad j = 1, \dots, n_{\mathbf{Y}} \quad (17)$$

$$\sum_{j=1}^{n_{\mathbf{Y}}+1} W^k(i, j) = 1, \quad i = 1, \dots, n_{\mathbf{X}} \quad (18)$$

$$W^k(n_{\mathbf{X}} + 1, n_{\mathbf{Y}} + 1) = 0, \quad (19)$$

where $W^k(i, j)$ is the (i, j) element of matrix W^k . A value $W^k(i, j) = 1$ means that \mathbf{x}_i^k is assigned to \mathbf{y}_j^k and a value $W^k(i, j) = 0$ means that \mathbf{x}_i^k is not assigned to \mathbf{y}_j^k . In addition, if \mathbf{x}_i^k is left without assignment, $W^k(i, n_{\mathbf{Y}} + 1) = 1$. Similarly, if \mathbf{y}_j^k is left without assignment, $W^k(n_{\mathbf{X}} + 1, j) = 1$. The set of binary matrices that meet (16)-(19) is $\mathcal{W}_{\mathbf{X}, \mathbf{Y}}$.

The linear programming T-GOSPA q-metric is based on changing the binary constraint (16) by a relaxed version

$$W^k(i, j) \geq 0, \quad \forall i, j. \quad (20)$$

The set of matrices that meet (17)-(19) and (20) is denoted as $\overline{\mathcal{W}}_{\mathbf{X}, \mathbf{Y}}$.

Proposition 9. *Given a base q-metric $d_b(\cdot, \cdot)$ in the single-object space \mathbb{X} , a maximum localisation cost $c > 0$, a real parameter p with $1 \leq p < \infty$, a track switching penalty $\gamma > 0$, and q-metric parameter $\rho \in (0, 1)$, the LP relaxation $\overline{d}_p^{(c, \rho, \gamma)}(\mathbf{X}, \mathbf{Y})$ of $d_p^{(c, \rho, \gamma)}(\mathbf{X}, \mathbf{Y})$ is a q-metric with expression*

$$\begin{aligned} \overline{d}_p^{(c, \rho, \gamma)}(\mathbf{X}, \mathbf{Y}) = & \min_{W^k \in \overline{\mathcal{W}}_{\mathbf{X}, \mathbf{Y}}} \left(\sum_{k=1}^T \text{tr}[(D_{\mathbf{X}, \mathbf{Y}}^k)^\dagger W^k] \right. \\ & \left. + \frac{\gamma^p}{2} \sum_{k=1}^{T-1} \sum_{i=1}^{n_{\mathbf{X}}} \sum_{j=1}^{n_{\mathbf{Y}}} |W^k(i, j) - W^{k+1}(i, j)| \right)^{\frac{1}{p}}, \end{aligned} \quad (21)$$

where $D_{\mathbf{X}, \mathbf{Y}}^k$ is a matrix of size $(n_{\mathbf{X}} + 1) \times (n_{\mathbf{Y}} + 1)$ whose (i, j) element is

$$D_{\mathbf{X}, \mathbf{Y}}^k(i, j) = d_p^{(c, \rho)}(\mathbf{x}_i^k, \mathbf{y}_j^k)^p \quad (22)$$

where we recall that $d_p^{(c, \rho)}(\cdot, \cdot)$ is the GOSPA q-metric (11), and $\mathbf{x}_{n_{\mathbf{X}}+1}^k = \emptyset$ and $\mathbf{y}_{n_{\mathbf{Y}}+1}^k = \emptyset$.

The identity property of the q-metric is direct and the triangle inequality is proved in Appendix C. It should be noted that if instead of optimising over $\overline{\mathcal{W}}_{\mathbf{X}, \mathbf{Y}}$ in (21), we optimise over $\mathcal{W}_{\mathbf{X}, \mathbf{Y}}$ (the non-relaxed assignment matrices), (21) becomes (12). In addition, as in [18], it is possible to add time weights in both (12) and (21) and the q-metric properties are preserved.

As the T-GOSPA metric, the T-GOSPA q-metric can be decomposed into different costs associated to localisation errors, missed objects, false objects and track switches [20, Sec. IV.C]. This decomposition provides a clear interpretability of the obtained results.

D. Examples

We illustrate how the T-GOSPA q-metric works for the examples shown in Figure 2. As before, we consider the case $p = 1$. For sufficiently small γ , estimate \mathbf{Y}_1 has five properly

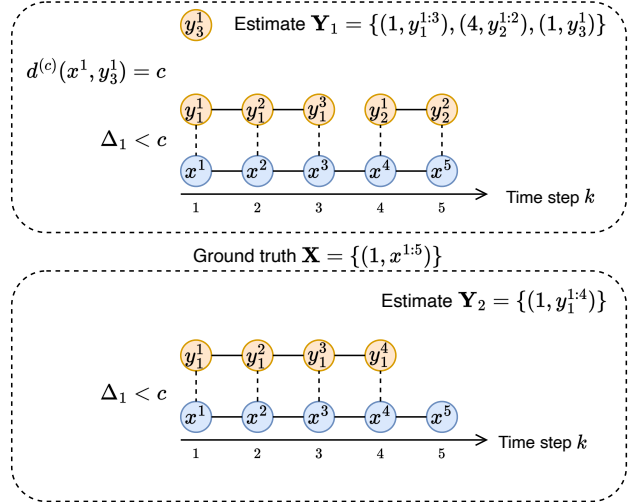


Figure 2: Two estimated sets of trajectories \mathbf{Y}_1 and \mathbf{Y}_2 of the ground truth \mathbf{X} . The dashed lines represent assignments between the elements of the ground truth and the estimate. Estimate \mathbf{Y}_1 has five correct detections with localisation error Δ_1 , a false object and a track switch. Estimate \mathbf{Y}_2 has four properly detected objects with localisation error Δ_1 and a missed object.

detected objects with localisation error Δ_1 , a false object and a track switch, resulting in the value

$$d_1^{(c, \rho)}(\mathbf{X}, \mathbf{Y}_1) = 5\Delta_1 + \rho c + \gamma. \quad (23)$$

It should be noted that, if γ were sufficiently high, the optimal assignments are fixed across time, and therefore the optimal assignment for \mathbf{Y}_1 would not be the one in Figure 2. In this case, it would be optimal to leave the trajectory $(4, y_2^{1:2})$ unassigned with an overall q-metric value $3\Delta_1 + \rho c + 2c$. That is, we substitute the localisation costs for two objects ($2\Delta_1$) plus the track switching cost γ in (23) by the cost of two missed objects and two false objects ($2c$), which would result in \mathbf{Y}_2 being always better than \mathbf{Y}_1 , regardless of ρ .

Therefore, for sufficiently small γ , the optimal assignment is the one in Figure 2 if

$$5\Delta_1 + \rho c + \gamma < 3\Delta_1 + \rho c + 2c \quad (24)$$

which implies that the track switching cost must meet

$$\gamma < 2(c - \Delta_1). \quad (25)$$

On the other hand, estimate \mathbf{Y}_2 has four properly detected objects with localisation error Δ_1 and a missed object, resulting in the value

$$d_1^{(c, \rho)}(\mathbf{X}, \mathbf{Y}_2) = 4\Delta_1 + (1 - \rho)c. \quad (26)$$

According to the T-GOSPA q-metric, the estimate \mathbf{Y}_2 is more accurate than \mathbf{Y}_1 if $d_1^{(c, \rho)}(\mathbf{X}, \mathbf{Y}_1) > d_1^{(c, \rho)}(\mathbf{X}, \mathbf{Y}_2)$, which is met if

$$\rho > \frac{c - \Delta_1 - \gamma}{2c}. \quad (27)$$

That is, the cost for false objects should be sufficiently high to penalise \mathbf{Y}_1 more than \mathbf{Y}_2 . For instance, let us consider $c = 1$, $\Delta_1 = 0.1$ and $\gamma = 0.1$. Then, estimate \mathbf{Y}_2 is more accurate than \mathbf{Y}_1 if $\rho > 0.4$. This implies that the T-GOSPA

metric ($\rho = 0.5$) indicates that \mathbf{Y}_2 is more accurate than \mathbf{Y}_1 . However, if $\rho < 0.4$, which implies that the cost for false objects ρ is smaller than the cost for missed objects $(1 - \rho)$, then estimate \mathbf{Y}_1 is more accurate than \mathbf{Y}_2 .

E. Properties

This section extends the properties of the GOSPA q-metric presented in Section III-D to the T-GOSPA q-metric. The following result holds directly from the definition.

Lemma 10. *If $d_b(\cdot, \cdot)$ is a metric, the T-GOSPA q-metric and its LP relaxation meet*

$$d_p^{(c, \rho, \gamma)}(\mathbf{X}, \mathbf{Y}) = d_p^{(c, 1-\rho, \gamma)}(\mathbf{Y}, \mathbf{X}) \quad (28)$$

$$\bar{d}_p^{(c, \rho, \gamma)}(\mathbf{X}, \mathbf{Y}) = \bar{d}_p^{(c, 1-\rho, \gamma)}(\mathbf{Y}, \mathbf{X}). \quad (29)$$

The following lemma regarding the optimal assignment is proved in Appendix D-A.

Lemma 11. *The optimal sequence of matrices $W^k \in \bar{\mathcal{W}}_{\mathbf{X}, \mathbf{Y}}$ with $k = 1, \dots, T$, in the LP T-GOSPA q-metric does not depend on ρ . Similarly, the optimal sequence of matrices $W^k \in \mathcal{W}_{\mathbf{X}, \mathbf{Y}}$ with $k = 1, \dots, T$ in the T-GOSPA q-metric does not depend on ρ .*

A direct consequence of this lemma is that the optimal sequence of assignment vectors $\pi^k \in \Pi_{\mathbf{X}, \mathbf{Y}}$, $k = 1, \dots, T$ of the T-GOSPA q-metric does not depend on ρ . Lemma 11 implies that for different values of ρ , the localisation and track switching costs remain unchanged, but there are different missed and false object costs. In addition, this implies that, if $d_b(\cdot, \cdot)$ is a metric, the optimal W^k is the same as in the T-GOSPA metric. If we want to compute the q-metric for several values of ρ , this lemma provides a computational advantage, as it suffices to solve the optimisation problem once.

The T-GOSPA q-metric symmetrisation property is provided in the following lemma (proved in Appendix D-B).

Lemma 12. *If $d_b(\cdot, \cdot)$ is a metric, the T-GOSPA metrics $d_p^{(c, 1/2, \gamma)}(\mathbf{X}, \mathbf{Y})$ and $\bar{d}_p^{(c, 1/2, \gamma)}(\mathbf{X}, \mathbf{Y})$ are recovered with the following symmetrisation of the TGOSPA q-metrics*

$$d_p^{(c, 1/2, \gamma)}(\mathbf{X}, \mathbf{Y}) = \left[\frac{1}{2} \left(d_p^{(c, \rho, \gamma)}(\mathbf{X}, \mathbf{Y})^p + d_p^{(c, \rho, \gamma)}(\mathbf{Y}, \mathbf{X})^p \right) \right]^{1/p}, \quad (30)$$

$$\bar{d}_p^{(c, 1/2, \gamma)}(\mathbf{X}, \mathbf{Y}) = \left[\frac{1}{2} \left(\bar{d}_p^{(c, \rho, \gamma)}(\mathbf{X}, \mathbf{Y})^p + \bar{d}_p^{(c, \rho, \gamma)}(\mathbf{Y}, \mathbf{X})^p \right) \right]^{1/p}. \quad (31)$$

V. Q-METRICS FOR RANDOM FINITE SETS

This section extends the GOSPA and T-GOSPA q-metrics to RFSs of objects [29] and trajectories [30]. This extension is relevant for performance evaluation via Monte Carlo simulations. It is also relevant for performance evaluation using a dataset containing multiple scenarios, each associated with a different ground truth. It is possible to understand these two cases as the comparison between an RFS with the ground truth and another RFS with the estimate [18, Sec. V].

A. RFS of objects

The GOSPA q-metric can be extended to RFSs of objects using the expected GOSPA q-metric value, as done for the GOSPA metric [13, Sec. III]. We consider a real parameter p' such that $1 \leq p' < \infty$. The expected value of the GOSPA q-metric to the p' power is

$$\mathbb{E}[d_p^{(c, \rho)}(\mathbf{x}, \mathbf{y})^{p'}] = \int \int d_p^{(c, \rho)}(\mathbf{x}, \mathbf{y})^{p'} p(\mathbf{x}, \mathbf{y}) \delta \mathbf{x} \delta \mathbf{y} \quad (32)$$

where this expectation is a double set integral [29] taken with respect to the joint density $p(\mathbf{x}, \mathbf{y})$ of the RFSs \mathbf{x} and \mathbf{y} .

Lemma 13. *For a real parameter p' such that $1 \leq p' < \infty$, $(\mathbb{E}[d_p^{(c, \rho)}(\mathbf{x}, \mathbf{y})^{p'}])^{1/p'}$ is a q-metric on the space of RFSs of objects with a finite cardinality moment $\mathbb{E}[|\cdot|^{p'/p}] < \infty$.*

The proof is equivalent to the proof of Proposition 2 in [13].

B. RFS of trajectories

Analogous to the T-GOSPA metric [20, Sec. V], we can extend the T-GOSPA q-metric to RFSs of trajectories using the expected T-GOSPA q-metric value. The expected value of the T-GOSPA q-metric to the p' power has the same expression as (32), but using \mathbf{X} and \mathbf{Y} instead of \mathbf{x} and \mathbf{y} , and sets integrals for sets of trajectories [30] instead of sets integrals for sets of objects.

Lemma 14. *For a real parameter p' such that $1 \leq p' < \infty$, $(\mathbb{E}[d_p^{(c, \rho)}(\mathbf{X}, \mathbf{Y})^{p'}])^{1/p'}$ is a q-metric on the space of RFSs of trajectories with a finite cardinality moment $\mathbb{E}[|\cdot|^{p'/p}] < \infty$.*

The proof is equivalent to the proof of Lemma 3 in [20].

VI. SIMULATIONS

This section examines the performance of several Bayesian MOT algorithms via the T-GOSPA q-metric via simulations. We have implemented the trajectory Poisson multi-Bernoulli mixture (T-PMBM) filter [32], the PMBM filter [33], [34] and the generalised labelled multi-Bernoulli (GLMB) filter [35]. The PMBM and GLMB both use sequential track formation by connecting state estimates with a similar auxiliary variable (PMBM) [36] or with the same label (GLMB). T-PMBM and PMBM consider a maximum number of 200 global hypothesis, while GLMB has a maximum of 1000 global hypotheses. All filters use Murty's algorithm [37] in the update step to select the global hypotheses, arising from a previous global hypotheses, that have the highest weights. The T-PMBM implementation uses an L -scan window with $L = 5$, to jointly update the last L time steps of single-trajectory densities. The pruning and estimation parameters are set as in [36]. All units are in the international system and are not explicitly stated for brevity.

The state of a single object is $x = [p_x, \dot{p}_x, p_y, \dot{p}_y]^T$, containing 2-D position $[p_x, p_y]^T$ and velocity $[\dot{p}_x, \dot{p}_y]^T$. Objects move with a nearly constant velocity model [38] with a sampling time $\tau = 1$, and the multiplication factor of the

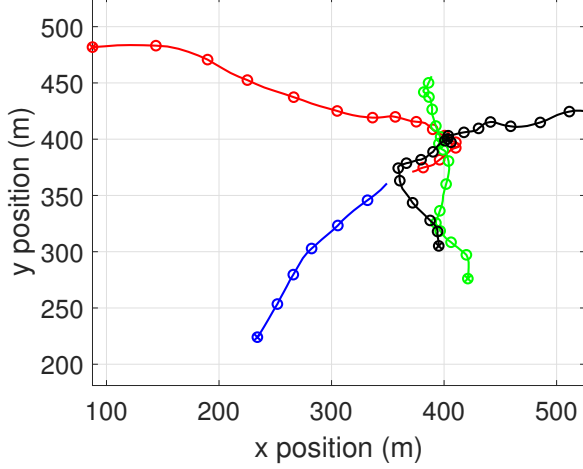


Figure 3: Scenario considered the simulations. All objects appear at time step 1 except the black one, which appears at time step 6. The initial object states are marked with a cross. The blue object dies at time step 30, the red at time step 75, the green at time step 80 and the black one at time step 100.

process noise covariance is $q = 0.4$. The probability of survival of the objects is 0.99.

The birth single-object density is $p_b(x) = \mathcal{N}(x; \bar{x}_b, P_b)$, which represents a Gaussian density with mean $\bar{x}_b = [400, 0, 400, 0]^T$ and covariance matrix $P_b = \text{diag}([300^2, 2^2, 300^2, 2^2])$. For T-PMBM and PMBM filters, the birth model is a Poisson point process (PPP). Its intensity is $3p_b(x)$ at the initial time step ($k = 1$) and $0.005p_b(x)$ at the following time steps. The GLMB filter uses a multi-Bernoulli birth model, which is chosen to approximate the PPP birth model with 5 Bernoulli components as in [36].

The probability of detection of each object is set to $p^D = 0.9$. The sensor measures the positional elements with an additive zero-mean Gaussian noise with covariance matrix $R = \text{diag}([4, 4])$. Clutter follows a PPP whose intensity is $\lambda^C(z) = \bar{\lambda}^C u_A(z)$ where $\bar{\lambda}^C = 20$ and $u_A(z)$ is a uniform density in the area $A = [0, 800] \times [0, 800]$. The simulation has 101 time steps and contains four objects. The scenario is represented in Figure 3. Three of these objects get in close proximity roughly at the middle of the simulation.

At each time step, we evaluate the accuracy of the estimated set $\hat{\mathbf{X}}_k$ of all trajectories (positional elements) up to the current time step k compared with the true set \mathbf{X}_k of all trajectories via Monte Carlo simulation with $N_{mc} = 100$ runs. The T-GOSPA q-metric has been implemented with the Euclidean distance, parameter $p = 2$, maximum localisation error $c = 10$, track switching penalty $\gamma = 1$ and q-metric parameter $\rho \in \{0.3, 0.5, 0.7\}$. We consider three choices of ρ to analyse the effect of this parameter in the q-metric value. With $\rho = 0.3$, missed objects are penalised more than false objects. With $\rho = 0.5$, missed and false objects are penalised equally (T-GOSPA metric). With $\rho = 0.7$, false objects are penalised more than missed objects. The root mean square (RMS) T-

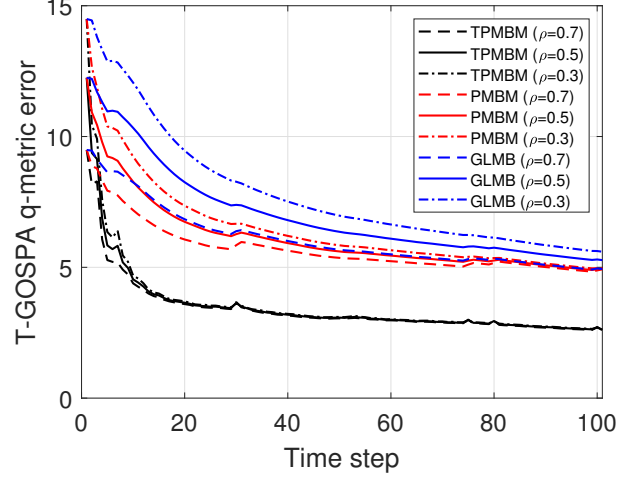


Figure 4: RMS-T-GOSPA q-metric errors at each time step. The TPMBM filter performs best for all considered values of ρ .

GOSPA q-metric at time step k is

$$d(k) = \sqrt{\frac{1}{N_{mc}k} \sum_{i=1}^{N_{mc}} d_2^{(10, \rho)}(\mathbf{X}_k, \hat{\mathbf{X}}_k^i)^2}, \quad (33)$$

where the squared q-metric has been normalised by the time window length k (the time window is from time step 1 to k). Equation (33) is a Monte Carlo approximation of the q-metric for RFSs in Lemma 14. In this case, \mathbf{X}_k can be considered a deterministic RFS, and $\hat{\mathbf{X}}_k^i$ are realisations of the estimated RFS of trajectories.

The RMS-T-GOSPA q-metric errors calculated at each time step are shown in Figure 4. For all choices of ρ , the T-PMBM filter achieves the best performance, followed in order by PMBM and GLMB. The q-metric errors are higher with $\rho = 0.3$ than with the other values of ρ . This means that in this scenario there are more missed objects than false objects, which can also be checked in the error decomposition in Figure 5. Overall, the q-metric value decreases with time since the estimation of all the trajectories becomes more accurate (normalised by the time window length). While localisation errors stay roughly the same across time, the missed object cost decreases since objects are mainly missed at the beginning of the simulation, so their normalised cost decreases with time. At the time steps when there are object deaths, there are some spikes in the T-GOSPA error, due to false alarms. We can see that the spikes are larger with $\rho = 0.7$ since higher ρ penalises false objects more. From Lemma 11, we know that the localisation error and track switching cost do not change with ρ . This can be seen in Figure 5.

We now proceed to evaluate tracking performance for different values of p^D and $\bar{\lambda}^C$. The RMS-GOSPA error across all time steps is shown in Table I. As space allows, this table also includes the (track-oriented) PMB filter [33] with sequential track building. The best performing filter is always the T-PMBM filter, followed by PMBM/PMB (depending on the scenario) and then followed by GLMB. As expected, higher clutter and lower p^D increase the error. In all these cases,

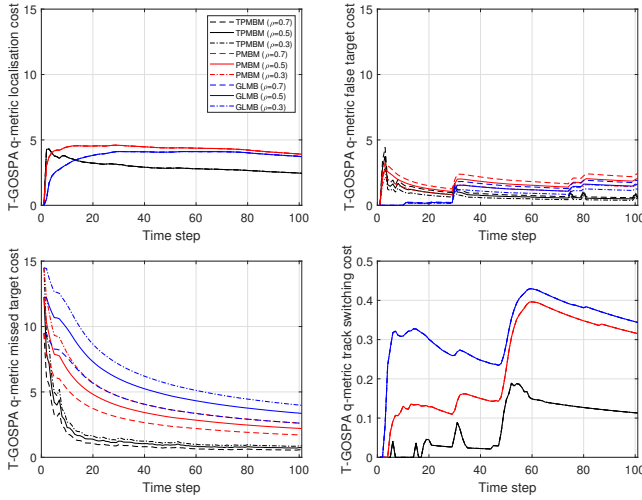


Figure 5: RMS-T-GOSPA q-metric decomposition across time. A change in ρ implies a change in the false and missed object costs, whereas localisation and track switching costs remain unchanged.

the missed object error dominates the false object error since q-metric value is highest for $\rho = 0.3$.

VII. CONCLUSIONS

This paper has presented two quasi-metrics for performance evaluation of multi-object tracking algorithms. The proposed quasi-metrics are extensions of the GOSPA metrics for sets of objects, and sets of trajectories, and allow uneven costs for the missed and false objects. The paper proves the identity and triangle inequality properties that are required to define quasi-metrics. The GOSPA and T-GOSPA quasi-metrics have also been extended to RFSs of objects and RFSs of trajectories.

The T-GOSPA q-metric has been applied to evaluate MOT simulation results for different values of ρ , showing the effects on the q-metric value of using different costs for missed and false objects. The GOSPA and T-GOSPA quasi-metrics should be used in applications in which the user is interested in penalising missed and false objects differently. This can be achieved by choosing the parameter ρ accordingly. In other cases, our recommendation for principled evaluation of MOT algorithms is to use the GOSPA and T-GOSPA metrics as well as their decompositions into their different components to provide a more thorough analysis.

A direction of future work is to extend the proposed quasi-metrics to uncertainty-aware MOT performance evaluation, as done for GOSPA and T-GOSPA in [39], [40].

REFERENCES

- [1] D. M. Jiménez-Bravo, A. Lozano Murciego, A. Sales Mendes, H. Sánchez San Blás, and J. Bajo, "Multi-object tracking in traffic environments: A systematic literature review," *Neurocomputing*, vol. 494, pp. 43–55, 2022.
- [2] P. Braca, P. Willett, K. LePage, S. Marano, and V. Matta, "Bayesian tracking in underwater wireless sensor networks with port-starboard ambiguity," *IEEE Transactions on Signal Processing*, vol. 62, no. 7, pp. 1864–1878, Apr. 2014.
- [3] E. Delande, J. Houssineau, J. Franco, C. Frueh, D. Clark, and M. Jah, "A new multi-target tracking algorithm for a large number of orbiting objects," *Advances in Space Research*, vol. 64, pp. 645–667, 2019.
- [4] S. Blackman and R. Popoli, *Design and Analysis of Modern Tracking Systems*. Artech House, 1999.
- [5] K. Smith, D. Gatica-Perez, J. Odobez, and S. Ba, "Evaluating multi-object tracking," in *IEEE Computer Society Conference on Computer Vision and Pattern Recognition*, 2005, pp. 36–36.
- [6] T. M. Apostol, *Mathematical Analysis*. Addison Wesley, 1974.
- [7] D. Schuhmacher and A. Xia, "A new metric between distributions of point processes," *Advances in Applied Probability*, vol. 40, no. 3, pp. 651–672, Sep. 2008.
- [8] D. Schuhmacher, B.-T. Vo, and B.-N. Vo, "A consistent metric for performance evaluation of multi-object filters," *IEEE Transactions on Signal Processing*, vol. 56, no. 8, pp. 3447–3457, Aug. 2008.
- [9] P. Barrios, M. Adams, K. Leung, F. Inostroza, G. Naqvi, and M. E. Orchard, "Metrics for evaluating feature-based mapping performance," *IEEE Transactions on Robotics*, vol. 33, no. 1, pp. 198–213, Feb. 2017.
- [10] P. Barrios and M. Adams, "A comparison of multi-object sub-pattern linear assignment metrics," in *12th International Conference on Control, Automation and Information Sciences*, 2023, pp. 712–718.
- [11] J. R. Hoffman and R. P. S. Mahler, "Multitarget miss distance via optimal assignment," *IEEE Transactions on Systems, Man, and Cybernetics - Part A: Systems and Humans*, vol. 34, no. 3, pp. 327–336, May 2004.
- [12] T. Vu, "A complete optimal subpattern assignment (CSPA) metric," in *23rd International Conference on Information Fusion*, 2020, pp. 1–8.
- [13] A. S. Rahmathullah, A. F. García-Fernández, and L. Svensson, "Generalized optimal sub-pattern assignment metric," in *20th International Conference on Information Fusion*, 2017, pp. 1–8.
- [14] K. Bernardin and R. Stiefelhagen, "Evaluating multiple object tracking performance: The CLEAR MOT metrics," *EURASIP Journal on Image and Video Processing*, vol. 2008, pp. 1–10, 2008.
- [15] H. Caesar et al., "nuScenes: A multimodal dataset for autonomous driving," in *IEEE/CVF Conference on Computer Vision and Pattern Recognition (CVPR)*, 2020, pp. 11 618–11 628.
- [16] J. Luiten et al., "HOTA: A higher order metric for evaluating multi-object tracking," *International Journal of Computer Vision*, pp. 1–31, 2020.
- [17] M. Beard, B. T. Vo, and B. Vo, "A solution for large-scale multi-object tracking," *IEEE Transactions on Signal Processing*, vol. 68, pp. 2754–2769, 2020.
- [18] A. F. García-Fernández, A. S. Rahmathullah, and L. Svensson, "A time-weighted metric for sets of trajectories to assess multi-object tracking algorithms," in *24th International Conference on Information Fusion*, 2021, pp. 1–8.
- [19] J. Bento and J. J. Zhu, "A metric for sets of trajectories that is practical and mathematically consistent," 2018. [Online]. Available: <https://arxiv.org/abs/1601.03094>
- [20] A. F. García-Fernández, A. S. Rahmathullah, and L. Svensson, "A metric on the space of finite sets of trajectories for evaluation of multi-target tracking algorithms," *IEEE Transactions on Signal Processing*, vol. 68, pp. 3917–3928, 2020.
- [21] V. N. Wernholm, A. Wärnsäter, and A. Ringh, "Fast computation of the TGOSPA metric for multiple target tracking via unbalanced optimal transport," *IEEE Control Systems Letters*, vol. 9, pp. 498–503, 2025.
- [22] M. Skolnik, *Introduction to Radar Systems*. McGraw-Hill, 2001.
- [23] W. A. Wilson, "On quasi-metric spaces," *American Journal of Mathematics*, vol. 53, no. 3, pp. 675–684, Jul. 1931.
- [24] V. Schroeder, "Quasi-metric and metric spaces," *Conformal Geometry and Dynamics*, vol. 10, pp. 355–360, Dec. 2006.
- [25] J. Bento and S. Ioannidis, "A family of tractable graph metrics," *Applied Network Science*, vol. 4, no. 107, 2019.
- [26] A. Stojmirović, "Quasi-metrics, similarities and searches: aspects of geometry of protein datasets," Ph.D. dissertation, Victoria University of Wellington, 2005.
- [27] T. Wang, A. Torralba, P. Isola, and A. Zhang, "Optimal goal-reaching reinforcement learning via quasimetric learning," in *Proceedings of the 40th International Conference on Machine Learning*, 2023, pp. 36 411–36 430.
- [28] T. Wang and P. Isola, "On the learning and learnability of quasimetrics," in *International Conference on Learning Representations*, 2022.
- [29] R. P. S. Mahler, *Advances in Statistical Multisource-Multitarget Information Fusion*. Artech House, 2014.
- [30] A. F. García-Fernández, L. Svensson, and M. R. Morelande, "Multiple target tracking based on sets of trajectories," *IEEE Transactions on Aerospace and Electronic Systems*, vol. 56, no. 3, pp. 1685–1707, Jun. 2020.
- [31] S. Yang, M. Baum, and K. Granström, "Metrics for performance evaluation of elliptic extended object tracking methods," in *IEEE*

Table I: RMS-TGOSPA q-metric errors across all time steps

p^D	$\bar{\lambda}^C$	T-PMBM $\rho =$			PMBM $\rho =$			PMB $\rho =$			GLMB $\rho =$		
		0.3	0.5	0.7	0.3	0.5	0.7	0.3	0.5	0.7	0.3	0.5	0.7
0.8	15	4.57	4.28	3.98	7.46	6.89	6.26	7.43	6.95	6.43	8.83	7.85	6.73
	20	4.79	4.50	4.18	7.64	7.03	6.36	7.61	7.10	6.55	9.13	8.09	6.90
	25	5.26	4.82	4.34	7.98	7.29	6.52	7.83	7.27	6.66	9.38	8.29	7.04
0.9	15	3.97	3.78	3.58	6.75	6.29	5.80	6.70	6.29	5.85	8.16	7.25	6.21
	20	4.08	3.84	3.59	6.84	6.34	5.80	6.78	6.34	5.86	8.35	7.39	6.29
	25	4.23	3.94	3.62	7.07	6.52	5.91	6.95	6.47	5.96	8.57	7.57	6.42
0.95	15	3.70	3.51	3.30	6.40	5.91	5.37	6.37	5.92	5.43	7.83	6.95	5.94
	20	3.70	3.51	3.32	6.43	5.93	5.38	6.40	5.95	5.46	7.98	7.06	6.00
	25	3.88	3.66	3.42	6.62	6.08	5.52	6.54	6.07	5.56	8.18	7.22	6.12

International Conference on Multisensor Fusion and Integration for Intelligent Systems, 2016, pp. 523–528.

- [32] K. Granström, L. Svensson, Y. Xia, J. Williams, and A. F. García-Fernández, “Poisson multi-Bernoulli mixtures for sets of trajectories,” *IEEE Transactions on Aerospace and Electronic Systems*, vol. 61, no. 2, pp. 5178–5194, 2025.
- [33] J. L. Williams, “Marginal multi-Bernoulli filters: RFS derivation of MHT, JIPDA and association-based MeMBer,” *IEEE Transactions on Aerospace and Electronic Systems*, vol. 51, no. 3, pp. 1664–1687, July 2015.
- [34] A. F. García-Fernández, J. L. Williams, K. Granström, and L. Svensson, “Poisson multi-Bernoulli mixture filter: direct derivation and implementation,” *IEEE Transactions on Aerospace and Electronic Systems*, vol. 54, no. 4, pp. 1883–1901, Aug. 2018.
- [35] B. T. Vo and B. N. Vo, “Labeled random finite sets and multi-object conjugate priors,” *IEEE Transactions on Signal Processing*, vol. 61, no. 13, pp. 3460–3475, July 2013.
- [36] A. F. García-Fernández, L. Svensson, J. L. Williams, Y. Xia, and K. Granström, “Trajectory Poisson multi-Bernoulli filters,” *IEEE Transactions on Signal Processing*, vol. 68, pp. 4933–4945, 2020.
- [37] K. G. Murty, “An algorithm for ranking all the assignments in order of increasing cost,” *Operations Research*, vol. 16, no. 3, pp. 682–687, 1968.
- [38] Y. Bar-Shalom, T. Kirubarajan, and X. R. Li, *Estimation with Applications to Tracking and Navigation*. John Wiley & Sons, Inc., 2001.
- [39] Y. Xia, A. F. García-Fernández, J. Karlsson, K.-C. Chang, T. Yuan, and L. Svensson, “Probabilistic GOSPA: a metric for performance evaluation of multi-object filters with uncertainties,” *accepted in IEEE Transactions on Aerospace and Electronic Systems*, 2025.
- [40] Y. Xia, A. F. García-Fernández, J. Karlsson, Y. Ge, L. Svensson, and T. Yuan, “Probabilistic trajectory GOSPA: A metric for uncertainty-aware multi-object tracking performance evaluation,” 2025. [Online]. Available: <https://arxiv.org/abs/2506.15148>
- [41] C. S. Kubrusly, *The Elements of Operator Theory*. Springer Science + Business Media, 2011.

Supplemental material: “GOSPA and T-GOSPA quasi-metrics for evaluation of multi-object tracking algorithms”

APPENDIX A

We prove the triangle inequality for the GOSPA q-metric. In particular we prove that for any set Z , the following inequality holds

$$d_p^{(c,\rho)}(X, Y) \leq d_p^{(c,\rho)}(X, Z) + d_p^{(c,\rho)}(Z, Y). \quad (34)$$

We proceed as in the proof of triangle inequality for the GOSPA metric [13, App. A].

The Minkowski's inequality for two sequences of different lengths (a_1, \dots, a_m) and (b_1, \dots, b_n) with $m \leq n$, and $1 \leq p \leq \infty$ is required in the proof and is given by [41]

$$\begin{aligned} & \left(\sum_{i=1}^m |a_i + b_i|^p + \sum_{i=m+1}^n |b_i|^p \right)^{1/p} \\ & \leq \left(\sum_{i=1}^m |a_i|^p + \sum_{i=1}^n |b_i|^p \right)^{1/p}. \end{aligned} \quad (35)$$

We first assume that $|Y| \geq |X|$ and consider three different cases depending on the cardinality of Z in relation to the cardinality of X and Y .

A. Case 1: $|X| \leq |Y| \leq |Z|$

For any $\pi \in \Pi_{|Y|}$, we have

$$\begin{aligned} & d_p^{(c,\rho)}(X, Y) \\ & \leq \left(\sum_{i=1}^{|X|} d^{(c)}(x_i, y_{\pi(i)})^p + \rho c^p (|Y| - |X|) \right)^{1/p}. \end{aligned} \quad (36)$$

Using the triangle inequality on the single-object q-metric, and any permutation $\sigma \in \Pi_{|Z|}$, we obtain

$$\begin{aligned} & d_p^{(c,\rho)}(X, Y) \\ & \leq \left(\sum_{i=1}^{|X|} \left[d^{(c)}(x_i, z_{\sigma(i)}) + d^{(c)}(z_{\sigma(i)}, y_{\pi(i)}) \right]^p \right. \\ & \quad \left. + \rho c^p (|Y| - |X|) \right)^{1/p} \\ & \leq \left(\sum_{i=1}^{|X|} \left[d^{(c)}(x_i, z_{\sigma(i)}) + d^{(c)}(z_{\sigma(i)}, y_{\pi(i)}) \right]^p \right. \\ & \quad \left. + \rho c^p (|Y| - |X|) + c^p (|Z| - |Y|) \right)^{1/p} \\ & = \left(\sum_{i=1}^{|X|} \left[d^{(c)}(x_i, z_{\sigma(i)}) + d^{(c)}(z_{\pi^{-1}(\sigma(i))}, y_i) \right]^p \right. \end{aligned}$$

$$\left. + \rho c^p (|Z| - |X|) + (1 - \rho) c^p (|Z| - |Y|) \right)^{1/p} \quad (37)$$

where π^{-1} is the inverse permutation of π . Now, we define the permutation $\tau \in \Pi_{|Z|}$ such that the first $|X|$ entries are $\pi^{-1}(\sigma(i))$ for $i = 1, \dots, |X|$. Then, we can write

$$\begin{aligned} & d_p^{(c,\rho)}(X, Y) \\ & \leq \left(\sum_{i=1}^{|X|} \left[d^{(c)}(x_i, z_{\sigma(i)}) + d^{(c)}(z_{\tau(i)}, y_i) \right]^p \right. \\ & \quad \left. + \rho c^p (|Z| - |X|) + (1 - \rho) c^p (|Z| - |Y|) \right. \\ & \quad \left. + \sum_{i=|X|+1}^{|Y|} d^{(c)}(z_{\tau(i)}, y_i)^p \right)^{1/p} \\ & \leq \left(\sum_{i=1}^{|X|} d^{(c)}(x_i, z_{\sigma(i)}) + \rho c^p (|Z| - |X|) \right)^{1/p} \\ & \quad + \left(\sum_{i=1}^{|Y|} d^{(c)}(z_{\tau(i)}, y_i) + (1 - \rho) c^p (|Z| - |Y|) \right)^{1/p} \end{aligned} \quad (38)$$

where the last inequality has been obtained using (35).

This inequality holds for any permutation σ and τ , including the ones that minimise the first term and the second term respectively. Therefore, this shows (34) for the considered case.

B. Case 2: $|X| \leq |Z| \leq |Y|$

We proceed as in Case 1. For any $\pi \in \Pi_{|Y|}$ and $\sigma \in \Pi_{|Z|}$, we have

$$\begin{aligned} & d_p^{(c,\rho)}(X, Y) \\ & \leq \left(\sum_{i=1}^{|X|} \left[d^{(c)}(x_i, z_{\sigma(i)}) + d^{(c)}(z_{\sigma(i)}, y_{\pi(i)}) \right]^p \right. \\ & \quad \left. + \rho c^p (|Y| - |X|) \right)^{1/p} \\ & = \left(\sum_{i=1}^{|X|} \left[d^{(c)}(x_i, z_{\sigma(i)}) + d^{(c)}(z_{\sigma(i)}, y_{\pi(i)}) \right]^p \right. \\ & \quad \left. + \rho c^p (|Z| - |X|) + \rho c^p (|Y| - |Z|) \right)^{1/p} \\ & \leq \left(\sum_{i=1}^{|X|} \left[d^{(c)}(x_i, z_{\sigma(i)}) + d^{(c)}(z_i, y_{\tau(i)}) \right]^p \right. \\ & \quad \left. + \sum_{i=|X|+1}^{|Z|} d^{(c)}(z_i, y_{\tau(i)})^p + \rho c^p (|Z| - |X|) \right. \\ & \quad \left. + \rho c^p (|Y| - |Z|) \right)^{1/p} \\ & \leq \left(\sum_{i=1}^{|X|} d^{(c)}(x_i, z_{\sigma(i)}) + \rho c^p (|Z| - |X|) \right)^{1/p} \end{aligned}$$

$$+ \left(\sum_{i=1}^{|Z|} d^{(c)}(z_i, y_{\tau(i)}) + \rho c^p (|Y| - |Z|) \right)^{1/p} \quad (39)$$

where $\tau \in \Pi_{|Y|}$ is a permutation such that the first $|X|$ entries are $\sigma^{-1}(\pi(i))$ for $i = 1, \dots, |X|$. As in the previous case, this holds for any permutation σ and τ , which shows (34) for the considered case.

C. Case 3: $|Z| \leq |X| \leq |Y|$

We now obtain

$$\begin{aligned} d_p^{(c,\rho)}(X, Y) &\leq \left(\sum_{i=1}^{|X|} d^{(c)}(x_i, y_{\pi(i)})^p + \rho c^p (|Y| - |X|) \right)^{1/p} \\ &\leq \left(\sum_{i=1}^{|Z|} d^{(c)}(x_i, y_{\pi(i)})^p + c^p (|X| - |Z|) \right. \\ &\quad \left. + \rho c^p (|Y| - |X|) \right)^{1/p} \end{aligned} \quad (40)$$

where we have used that $d^{(c)}(x_i, y_{\pi(i)})^p \leq c^p$ for $i = |Z| + 1, \dots, |X|$. Then we obtain

$$\begin{aligned} d_p^{(c,\rho)}(X, Y) &\leq \left(\sum_{i=1}^{|Z|} d^{(c)}(x_i, y_{\pi(i)})^p + (1 - \rho) c^p (|X| - |Z|) \right. \\ &\quad \left. + \rho c^p (|Y| - |Z|) \right)^{1/p} \\ &\leq \left(\sum_{i=1}^{|Z|} \left[d^{(c)}(x_i, z_{\sigma(i)}) + d^{(c)}(z_{\sigma(i)}, y_{\pi(i)}) \right]^p \right. \\ &\quad \left. + (1 - \rho) c^p (|X| - |Z|) + \rho c^p (|Y| - |Z|) \right)^{1/p}. \end{aligned} \quad (41)$$

Proceeding as in the previous case, we prove the triangle inequality for this case.

D. Case 4: $|Y| \leq |X|$

The previous three cases show the triangle inequality for $|X| \leq Y$ for any $\rho \in (0, 1)$. If $|Y| \leq |X|$ and using Lemma (5), we have that

$$\begin{aligned} d_p^{(c,\rho)}(X, Y) &= d_p^{(c,1-\rho)}(Y, X) \\ &\leq d_p^{(c,1-\rho)}(Y, Z) + d_p^{(c,1-\rho)}(Z, X) \\ &= d_p^{(c,\rho)}(Z, Y) + d_p^{(c,\rho)}(X, Z) \end{aligned} \quad (42)$$

where in the second step we have used the previous derivation of the triangle inequality. This finishes the proof of the triangle inequality of the GOSPA q-metric.

APPENDIX B

This appendix contains the proofs of Lemmas 6 and 7 related to the GOSPA q-metric.

A. Proof of Lemma 6

In this appendix, we prove Lemma 6. We consider the case $|\mathbf{y}| \geq |\mathbf{x}|$ and, using (3), we write the optimal permutation as

$$\pi^* = \arg \min_{\pi \in \Pi_{|\mathbf{y}|}} \left(\sum_{i=1}^{|\mathbf{x}|} d^{(c)}(x_i, y_{\pi(i)})^p + \rho c^p (|\mathbf{y}| - |\mathbf{x}|) \right) \quad (43)$$

$$= \arg \min_{\pi \in \Pi_{|\mathbf{y}|}} \left(\sum_{i=1}^{|\mathbf{x}|} d^{(c)}(x_i, y_{\pi(i)})^p \right) \quad (44)$$

where we removed the second term as it does not depend on π . Thus, the optimal permutation π^* and consequently the optimal assignment do not depend on ρ . The proof for the case $|\mathbf{y}| \leq |\mathbf{x}|$ is analogous.

B. Proof of Lemma 7

In this appendix, we prove Lemma 7. We provide the proof for $|\mathbf{y}| \geq |\mathbf{x}|$, as the proof for $|\mathbf{y}| < |\mathbf{x}|$ follows similar steps. From (3), the GOSPA q-metric to the p -th power is

$$d_p^{(c,\rho)}(\mathbf{x}, \mathbf{y})^p = \rho c^p (|\mathbf{y}| - |\mathbf{x}|) + \min_{\pi \in \Pi_{|\mathbf{y}|}} \sum_{i=1}^{|\mathbf{x}|} d^{(c)}(x_i, y_{\pi(i)})^p. \quad (45)$$

In addition, using Lemma 5, $d_p^{(c,\rho)}(\mathbf{y}, \mathbf{x}) = d_p^{(c,1-\rho)}(\mathbf{x}, \mathbf{y})$. Therefore,

$$\begin{aligned} d_p^{(c,\rho)}(\mathbf{y}, \mathbf{x})^p &= (1 - \rho) c^p (|\mathbf{y}| - |\mathbf{x}|) \\ &\quad + \min_{\pi \in \Pi_{|\mathbf{y}|}} \sum_{i=1}^{|\mathbf{x}|} d^{(c)}(x_i, y_{\pi(i)})^p. \end{aligned} \quad (46)$$

Substituting the above two equations in (10), we obtain the GOSPA metric $d_p^{(c,1/2)}(\mathbf{x}, \mathbf{y})$ proving Lemma 6.

APPENDIX C

This appendix sketches the proof of the triangle inequality for the T-GOSPA q-metric in LP form (21). The proof is analogous for the T-GOSPA metric [20, App. B] so we mainly highlight the differences here. The proof for the multi-dimensional assignment form is similar [20, App. B].

Let $\bar{d}_p^{(c,\rho,\gamma)}(\mathbf{X}, \mathbf{Y}, W^{1:T})$ denote the T-GOSPA q-metric function in (21) as a function of the sequence of matrices $W^{1:T} = (W^1, \dots, W^T)$. Let $W_{\mathbf{X},\mathbf{Z}}^{\star,k}$ and $W_{\mathbf{Z},\mathbf{Y}}^{\star,k}$ be the matrices that minimise $\bar{d}_p^{(c,\rho,\gamma)}(\mathbf{Y}, \mathbf{Z}, W^{1:T})$ and $\bar{d}_p^{(c,\rho,\gamma)}(\mathbf{Z}, \mathbf{Y}, W^{1:T})$. Using the matrices $W_{\mathbf{X},\mathbf{Z}}^{\star,k}$ and $W_{\mathbf{Z},\mathbf{Y}}^{\star,k}$, we build a matrix $W_{\mathbf{X},\mathbf{Y}}^k$ that meets

$$W_{\mathbf{X},\mathbf{Y}}^k(i, j) = \sum_{l=1}^{n_Z} W_{\mathbf{X},\mathbf{Z}}^{\star,k}(i, l) W_{\mathbf{Z},\mathbf{Y}}^{\star,k}(l, j) \quad (47)$$

for $i \in \{1, \dots, n_{\mathbf{X}}\}$ and $j \in \{1, \dots, n_{\mathbf{Y}}\}$. The other entries of $W_{\mathbf{X}, \mathbf{Y}}^k$ are

$$W_{\mathbf{X}, \mathbf{Y}}^k(i, j) = \begin{cases} 1 - \sum_{j=1}^{n_{\mathbf{Y}}} W_{\mathbf{X}, \mathbf{Y}}^k(i, j) & i \in \{1, \dots, n_{\mathbf{X}}\}, j = n_{\mathbf{Y}} + 1 \\ 1 - \sum_{i=1}^{n_{\mathbf{X}}} W_{\mathbf{X}, \mathbf{Y}}^k(i, j) & i = n_{\mathbf{X}} + 1, j \in \{1, \dots, n_{\mathbf{Y}}\} \\ 0 & i = n_{\mathbf{X}} + 1, j = n_{\mathbf{Y}} + 1. \end{cases} \quad (48)$$

Then, it can be shown that

$$\bar{d}_p^{(c, \rho, \gamma)}(\mathbf{X}, \mathbf{Y}, W_{\mathbf{X}, \mathbf{Y}}^{1:T}) \leq \bar{d}_p^{(c, \rho, \gamma)}(\mathbf{X}, \mathbf{Z}) + \bar{d}_p^{(c, \rho, \gamma)}(\mathbf{Z}, \mathbf{Y}). \quad (49)$$

Proving this result directly shows the triangle inequality as, by definition, $\bar{d}_p^{(c, \rho, \gamma)}(\mathbf{X}, \mathbf{Y}) \leq \bar{d}_p^{(c, \rho, \gamma)}(\mathbf{X}, \mathbf{Y}, W_{\mathbf{X}, \mathbf{Y}}^{1:T})$. The proof requires the use of two inequalities, one for the localisation cost, and another one for the track switching cost, which are then combined. Then, one applies the Minkowski inequality to the result. The track switching inequality in [20, Eq. (33)] holds, as the switching cost is the same in the metric and q-metric. The combination of both inequalities using the Minkowski inequality is also the same. The localisation cost inequality [20, Eq. (46)] only requires the following conditions: triangle inequality of the base q-metric, $D_{\mathbf{X}, \mathbf{Y}}^k(n_{\mathbf{X}} + 1, j) = D_{\mathbf{Z}, \mathbf{Y}}^k(n_{\mathbf{Z}} + 1, j)$ and $D_{\mathbf{X}, \mathbf{Y}}^k(i, n_{\mathbf{Y}} + 1) = D_{\mathbf{X}, \mathbf{Z}}^k(i, n_{\mathbf{Z}} + 1)$. All these properties are also met in the T-GOSPA q-metric, which implies that (49) holds, and the triangle inequality holds.

If we used time-weights in the definition of the T-GOSPA q-metric, the proof would be analogous to the one in [18].

APPENDIX D

In this appendix, we prove Lemmas 11 and 12 related to the T-GOSPA q-metric.

A. Proof of Lemma 11

In this appendix, we prove Lemma 11. In the cost function in (21), the only term that depends on ρ is $\text{tr}[(D_{\mathbf{X}, \mathbf{Y}}^k)^\dagger W^k]$ that can be written as

$$\begin{aligned} \text{tr}[(D_{\mathbf{X}, \mathbf{Y}}^k)^\dagger W^k] &= \sum_{i=1}^{n_{\mathbf{X}}+1} \sum_{j=1}^{n_{\mathbf{Y}}+1} W^k(i, j) D_{\mathbf{X}, \mathbf{Y}}^k(i, j) \\ &= \sum_{i=1}^{n_{\mathbf{X}}} \sum_{j=1}^{n_{\mathbf{Y}}} W^k(i, j) D_{\mathbf{X}, \mathbf{Y}}^k(i, j) \\ &\quad + \sum_{j=1}^{n_{\mathbf{Y}}} W^k(n_{\mathbf{X}} + 1, j) D_{\mathbf{X}, \mathbf{Y}}^k(n_{\mathbf{X}} + 1, j) \\ &\quad + \sum_{i=1}^{n_{\mathbf{X}}} W^k(i, n_{\mathbf{Y}} + 1) D_{\mathbf{X}, \mathbf{Y}}^k(i, n_{\mathbf{Y}} + 1). \end{aligned} \quad (50)$$

We now expand these sums over the cases where $\mathbf{x}_i^k \neq \emptyset$, $\mathbf{x}_i^k = \emptyset$, $\mathbf{y}_j^k \neq \emptyset$ and $\mathbf{y}_j^k = \emptyset$. In addition, we use the corresponding

value of $D_{\mathbf{X}, \mathbf{Y}}^k(i, j)$, see (22), when at least one of these sets is empty. This yields

$$\begin{aligned} \text{tr}[(D_{\mathbf{X}, \mathbf{Y}}^k)^\dagger W^k] &= \sum_{i=1: \mathbf{x}_i^k \neq \emptyset}^{n_{\mathbf{X}}} \sum_{j=1: \mathbf{y}_j^k \neq \emptyset}^{n_{\mathbf{Y}}} W^k(i, j) D_{\mathbf{X}, \mathbf{Y}}^k(i, j) \\ &\quad + \rho c^p \sum_{i=1: \mathbf{x}_i^k = \emptyset}^{n_{\mathbf{X}}} \sum_{j=1: \mathbf{y}_j^k \neq \emptyset}^{n_{\mathbf{Y}}} W^k(i, j) \\ &\quad + (1 - \rho) c^p \sum_{i=1: \mathbf{x}_i^k \neq \emptyset}^{n_{\mathbf{X}}} \sum_{j=1: \mathbf{y}_j^k = \emptyset}^{n_{\mathbf{Y}}} W^k(i, j) \\ &\quad + \rho c^p \sum_{j=1: \mathbf{y}_j^k \neq \emptyset}^{n_{\mathbf{Y}}} W^k(n_{\mathbf{X}} + 1, j) \\ &\quad + (1 - \rho) c^p \sum_{i=1: \mathbf{x}_i^k \neq \emptyset}^{n_{\mathbf{X}}} W^k(i, n_{\mathbf{Y}} + 1). \end{aligned} \quad (51)$$

Now, we use (18) and (19) to remove $W^k(n_{\mathbf{X}} + 1, j)$ and $W^k(i, n_{\mathbf{Y}} + 1)$ from the previous equation. By simplifying and rearranging the terms, we obtain

$$\begin{aligned} \text{tr}[(D_{\mathbf{X}, \mathbf{Y}}^k)^\dagger W^k] &= \sum_{i=1: \mathbf{x}_i^k \neq \emptyset}^{n_{\mathbf{X}}} \sum_{j=1: \mathbf{y}_j^k \neq \emptyset}^{n_{\mathbf{Y}}} W^k(i, j) D_{\mathbf{X}, \mathbf{Y}}^k(i, j) \\ &\quad + \sum_{j=1: \mathbf{y}_j^k \neq \emptyset}^{n_{\mathbf{Y}}} \rho c^p + \sum_{i=1: \mathbf{x}_i^k \neq \emptyset}^{n_{\mathbf{X}}} (1 - \rho) c^p \\ &\quad + \rho c^p \sum_{i=1: \mathbf{x}_i^k = \emptyset}^{n_{\mathbf{X}}} \sum_{j=1: \mathbf{y}_j^k \neq \emptyset}^{n_{\mathbf{Y}}} W^k(i, j) \\ &\quad - \rho c^p \sum_{j=1: \mathbf{y}_j^k \neq \emptyset}^{n_{\mathbf{Y}}} \sum_{i=1}^{n_{\mathbf{X}}} W^k(i, j) \\ &\quad + (1 - \rho) c^p \sum_{i=1: \mathbf{x}_i^k \neq \emptyset}^{n_{\mathbf{X}}} \sum_{j=1: \mathbf{y}_j^k = \emptyset}^{n_{\mathbf{Y}}} W^k(i, j) \\ &\quad - (1 - \rho) c^p \sum_{i=1: \mathbf{x}_i^k \neq \emptyset}^{n_{\mathbf{X}}} \sum_{j=1}^{n_{\mathbf{Y}}} W^k(i, j). \end{aligned} \quad (52)$$

We can simplify the third and fourth line, and the fifth and sixth line as follows

$$\begin{aligned} \text{tr}[(D_{\mathbf{X}, \mathbf{Y}}^k)^\dagger W^k] &= \sum_{i=1: \mathbf{x}_i^k \neq \emptyset}^{n_{\mathbf{X}}} \sum_{j=1: \mathbf{y}_j^k \neq \emptyset}^{n_{\mathbf{Y}}} W^k(i, j) D_{\mathbf{X}, \mathbf{Y}}^k(i, j) \\ &\quad + \sum_{j=1: \mathbf{y}_j^k \neq \emptyset}^{n_{\mathbf{Y}}} \rho c^p + \sum_{i=1: \mathbf{x}_i^k \neq \emptyset}^{n_{\mathbf{X}}} (1 - \rho) c^p \\ &\quad - \rho c^p \sum_{j=1: \mathbf{y}_j^k \neq \emptyset}^{n_{\mathbf{Y}}} \sum_{i=1: \mathbf{x}_i^k \neq \emptyset}^{n_{\mathbf{X}}} W^k(i, j) \\ &\quad - (1 - \rho) c^p \sum_{i=1: \mathbf{x}_i^k \neq \emptyset}^{n_{\mathbf{X}}} \sum_{j=1: \mathbf{y}_j^k \neq \emptyset}^{n_{\mathbf{Y}}} W^k(i, j). \end{aligned} \quad (53)$$

Summing the last two lines, we obtain

$$\begin{aligned}
\text{tr}[(D_{\mathbf{X},\mathbf{Y}}^k)^\dagger W^k] &= \sum_{i=1:\mathbf{x}_i^k \neq \emptyset}^{n_{\mathbf{X}}} \sum_{j=1:\mathbf{y}_j^k \neq \emptyset}^{n_{\mathbf{Y}}} W^k(i, j) D_{\mathbf{X},\mathbf{Y}}^k(i, j) \\
&+ \sum_{j=1:\mathbf{y}_j^k \neq \emptyset}^{n_{\mathbf{Y}}} \rho c^p + \sum_{i=1:\mathbf{x}_i^k \neq \emptyset}^{n_{\mathbf{X}}} (1 - \rho) c^p \\
&- c^p \sum_{j=1:\mathbf{y}_j^k \neq \emptyset}^{n_{\mathbf{Y}}} \sum_{i=1:\mathbf{x}_i^k \neq \emptyset}^{n_{\mathbf{X}}} W^k(i, j). \quad (54)
\end{aligned}$$

We can see that the only terms that depend on ρ are those in the second line. In the first line $D_{\mathbf{X},\mathbf{Y}}^k(i, j)$ does not depend on ρ since objects exist. Plugging (54) into (21), the terms that depend on ρ can be taken out of the optimisation function, and the optimisation function does not depend on ρ . This completes the proof of Lemma 11. Note that this proof is valid for the LP T-GOSPA q-metric and also for the T-GOSPA q-metric (without LP relaxation).

B. Proof of Lemma 12

In this appendix, we prove Lemma 12. Plugging (54) into (21), we obtain

$$\begin{aligned}
&\bar{d}_p^{(c,\rho,\gamma)}(\mathbf{X}, \mathbf{Y}) \\
&= \sum_{k=1}^T \left[\sum_{j=1:\mathbf{y}_j^k \neq \emptyset}^{n_{\mathbf{Y}}} \rho c^p + \sum_{i=1:\mathbf{x}_i^k \neq \emptyset}^{n_{\mathbf{X}}} (1 - \rho) c^p \right] \\
&+ \min_{\substack{W^k \in \mathcal{W}_{\mathbf{X},\mathbf{Y}} \\ k=1,\dots,T}} \left(\sum_{k=1}^T \left[\sum_{i=1:\mathbf{x}_i^k \neq \emptyset}^{n_{\mathbf{X}}} \sum_{j=1:\mathbf{y}_j^k \neq \emptyset}^{n_{\mathbf{Y}}} W^k(i, j) D_{\mathbf{X},\mathbf{Y}}^k(i, j) \right. \right. \\
&\quad \left. \left. - c^p \sum_{j=1:\mathbf{y}_j^k \neq \emptyset}^{n_{\mathbf{Y}}} \sum_{i=1:\mathbf{x}_i^k \neq \emptyset}^{n_{\mathbf{X}}} W^k(i, j) \right] \right) \\
&+ \frac{\gamma^p}{2} \sum_{k=1}^{T-1} \sum_{i=1}^{n_{\mathbf{X}}} \sum_{j=1}^{n_{\mathbf{Y}}} |W^k(i, j) - W^{k+1}(i, j)| \Big)^{\frac{1}{p}}. \quad (55)
\end{aligned}$$

Using Lemma 10, $\bar{d}_p^{(c,\rho,\gamma)}(\mathbf{Y}, \mathbf{X}) = \bar{d}_p^{(c,1-\rho,\gamma)}(\mathbf{X}, \mathbf{Y})$ and therefore

$$\begin{aligned}
&\bar{d}_p^{(c,\rho,\gamma)}(\mathbf{Y}, \mathbf{X}) \\
&= \sum_{k=1}^T \left[\sum_{j=1:\mathbf{y}_j^k \neq \emptyset}^{n_{\mathbf{Y}}} (1 - \rho) c^p + \sum_{i=1:\mathbf{x}_i^k \neq \emptyset}^{n_{\mathbf{X}}} \rho c^p \right] \\
&+ \min_{\substack{W^k \in \mathcal{W}_{\mathbf{X},\mathbf{Y}} \\ k=1,\dots,T}} \left(\sum_{k=1}^T \left[\sum_{i=1:\mathbf{x}_i^k \neq \emptyset}^{n_{\mathbf{X}}} \sum_{j=1:\mathbf{y}_j^k \neq \emptyset}^{n_{\mathbf{Y}}} W^k(i, j) D_{\mathbf{X},\mathbf{Y}}^k(i, j) \right. \right. \\
&\quad \left. \left. - c^p \sum_{j=1:\mathbf{y}_j^k \neq \emptyset}^{n_{\mathbf{Y}}} \sum_{i=1:\mathbf{x}_i^k \neq \emptyset}^{n_{\mathbf{X}}} W^k(i, j) \right] \right) \\
&+ \frac{\gamma^p}{2} \sum_{k=1}^{T-1} \sum_{i=1}^{n_{\mathbf{X}}} \sum_{j=1}^{n_{\mathbf{Y}}} |W^k(i, j) - W^{k+1}(i, j)| \Big)^{\frac{1}{p}}. \quad (56)
\end{aligned}$$

Substituting the above two equations in (31), we obtain the (LP) T-GOSPA metric $\bar{d}_p^{(c,1/2,\gamma)}(\mathbf{X}, \mathbf{Y})$. The same result can be obtained equivalently for $d_p^{(c,1/2,\gamma)}(\mathbf{X}, \mathbf{Y})$ proving Lemma 12.